Dalton Transactions

Accepted Manuscript

ROYAL SOCIETY OF CHEMISTRY

www.rsc.org/dalton

Cite this: DOI: 10.1039/c0xx00000x

www.rsc.org/xxxxxx

ARTICLE TYPE

Construction of covalent- and hydrogen-bonded assemblies from 1′,1‴-biferrocenediboronic acid as a new organobimetallic building block

Keishiro Tahara,[a]* Tetsuhiro Akita,[a] Shohei Katao,[a] Ken Tokunaga[b] and Jun-ichi Kikuchi[a]*

Received (in XXX, XXX) Xth XXXXXXXXX 20XX, Accepted Xth XXXXXXXXX 20XX

DOI: 10.1039/b000000x

1′,1‴-Biferrocenediboronic acid (**1**) was synthesized from 1′,1‴-dibromobiferrocene by a typical procedure of converting Br to $B(OH)_2$ groups in 76% yield and identified by ^{1}H-, ^{13}C- and ^{11}B-NMR and ESI-MS. X-ray diffraction (XRD) studies showed that, in non-solvated crystals (Form I), the new organobimetallic building block **1** formed 1D hydrogen-bonded networks (*i.e.*, chain) with octaatomic rings composed of the neighbouring two molecules. In solvated crystals with a composition of $(\mathbf{1})_3(THF)_2$ (Form II), **1** exists in two conformers (Conformers A and B) with respect to the rotation of the $CpB(OH)_2$ moieties relative to the Cp rings of the fulvalenide moieties; Conformer A formed 1D hydrogen-bonded networks laterally hydrogen-bonding with THF molecules while Conformer B formed a new planar hydrogen-bonded motif involving four $B(OH)_2$ groups and stepwise laminated networks of the planar motif. A macrocyclic tetraferrocenyl boronate ester **2** was synthesized by cyclocondensation between **1** and pentaerythritol in 33% yield and identified by ^{1}H-, ^{13}C- and ^{11}B-NMR, ESI-MS and XRD. In electrochemical measurements, the cyclocondensed compound **2** exhibited four defined reversible waves with a total spread of 756 mV in CH_2Cl_2 containing *n*-Bu_4NBArF_4 (ArF = 3,5-bis(trifluoromethyl)phenyl), displaying both intra- and inter-biferrocenyl interactions.

Introduction

The establishment of methodologies for spatial arrangement of metal ions or metal complexes with organic ligands is a basis for fabrication of functional metal organic frameworks (MOFs) and discrete multimetallic complexes.[1] Especially, the construction of multimetallic assemblies from bimetallic complexes is required in the field of molecular electronics for realization of a quantum cellular automaton (QCA),[2] where bimetallic mixed-valence complexes having two charge configurations are used as building blocks, or "cells". Although several theoretical models for QCA devices have been reported,[3] the molecular expression for QCA has still not been developed, primarily because of the limited methods for construction of assemblies from mixed-valence complexes.[4] To address this, a new synthetic strategy using two types of ligands is required, so that the first ligands chelate two metal ions to afford a bimetallic complex and the second ligands covalently or non-covalently connect the bimetallic complexes to afford the desired multimetallic assemblies.

Use of boronic acids is an effective tool in materials and supramolecular chemistry.[5] Multiple boronic acids are used for assemblies of 3D-expanded boroxines and boronate esters, such as covalent organic frameworks (COFs),[5b-d, 6] linear polymers[7] and discrete macrocycles,[8] as well as hydrogen-bonded networks.[9] Because they give unique sandwich-like geometries and electrochemical functions, these covalent and non-covalent methods have been applied to ferrocene (Fc) derivatives such as ferroceneboronic acid (**A**)[10] and 1,1′-ferrocenediboronic acid (**B**).[11] Based on the pioneering works using **B** to form hydrogen-bonded networks[11a] and multi-ferrocenyl compounds such as a macrocyclic ester,[11b] the biferrocene (BiFc) counterparts of diboronic acids are expected to be useful building blocks from the viewpoint of synthetic and supramolecular chemistry, as well as for a molecular QCA, because of the well-known iron-iron coupling properties of BiFc derivatives.[12] However, to the best of our knowledge, biferrocenyl boronic acids have not been reported. Furthermore, although there have been a number of reports on the synthesis of BiFc derivatives,[12] few attempts to construct covalent or non-covalent assemblies from BiFc building blocks have been reported.[13] To explore a new synthetic method, we report herein the first synthesis of 1′,1‴-biferrocenediboronic acid (**1**) and demonstrate the usefulness of **1** as a new organobimetallic building block for the construction of covalent and non-covalent assemblies (Scheme 1).

Results and discussion

Synthesis and characterization of 1

The new BiFc derivative **1** was designed to have bicyclopentadienyl (CpCp, fulvalenide) and functionalized cyclopentadienyl ($CpB(OH)_2$) rings as the first and second ligands, respectively (Scheme 1). **1** was synthesized from 1′,1‴-dibromobiferrocene[14] by a typical procedure of converting Br to $B(OH)_2$ groups with *n*-butyllithium followed by addition of tributyl borate and hydrolysis.[5a] The obtained compound **1** was

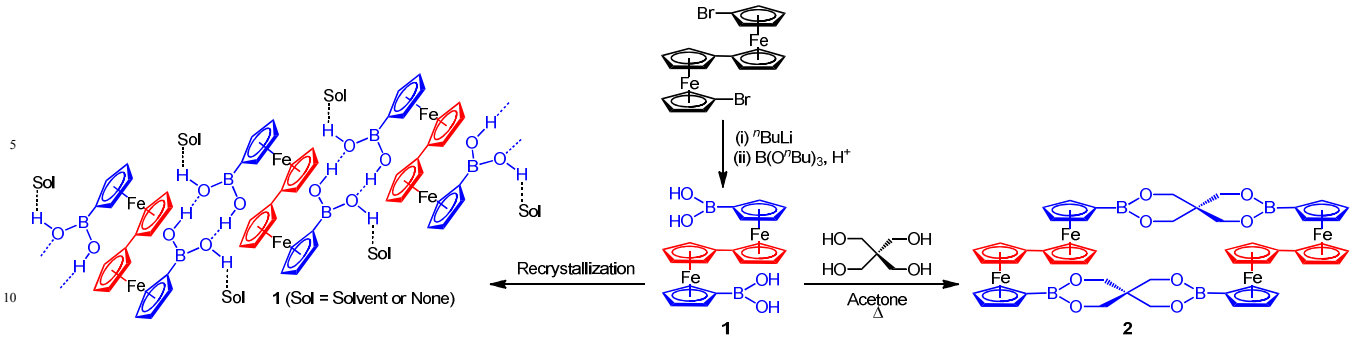

Scheme 1. Syntheses of 1′,1‴-biferrocenediboronic acid (**1**), 1D hydrogen-bonded networks and macrocyclic dimer (**2**). Red and blue moieties indicate the first and second ligands, respectively.

identified by ^{1}H- and ^{13}C-NMR and ESI-MS (Figs. S1-3). Four pseudo triplet peaks for the cyclopentadienyl (Cp) rings characteristic of 1′,1‴-disubstituted BiFc derivatives[12] were observed in the ^{1}H-NMR spectrum of **1** in DMSO-d_6, as shown in Fig. S2. A characteristic hydroxyl proton peak of B(OH)$_2$ groups was also observed at 7.37 ppm. In accordance with this, a characteristic peak for the boronic acid form was observed in the ^{11}B-NMR spectrum of **1** in DMSO-d_6 (29.0 ppm), whose chemical shift is comparable to that of **B** (29.07 ppm).[11c]

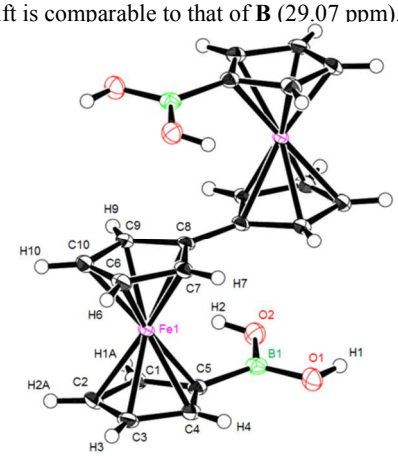

Fig. 1 ORTEP drawing of molecular structure of **1** in the crystal of Form I with thermal ellipsoids set at the 50% probability level. Selected bond lengths (Å) and angles (deg): O1-B1 1.361(3), O2-B1 1.381(3), C5-B1 1.555(3), C8-C8^1 1.461 (3), O1-B1-C5 120.33(19), O2-B1-C5 121.23(18), O1-B1-O2 118.42(16).

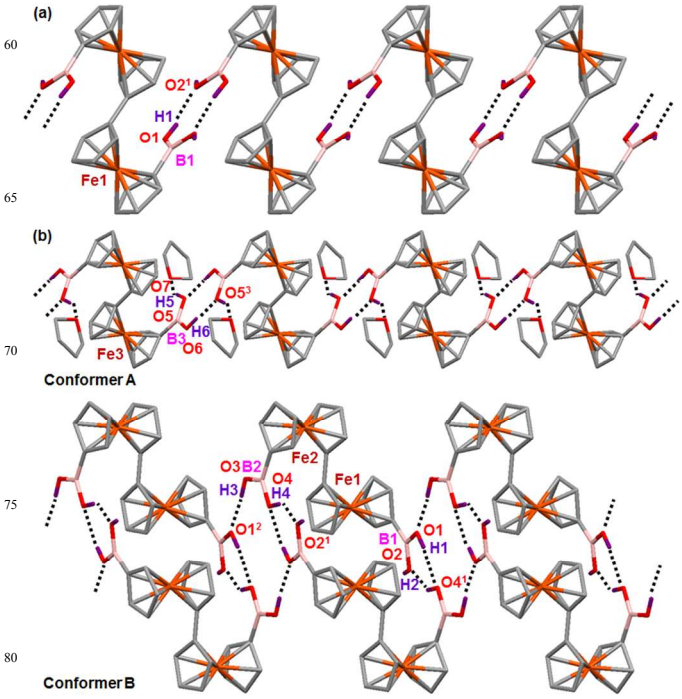

Fig. 2 (a) Hydrogen-bonded network of **1** in crystals of Form I and (b) networks composed of Conformers A and B of **1** in crystals of Form II. Hydrogen atoms are omitted for clarity expect for the O-H hydrogen atoms (purple). Hydrogen bonds are indicated as dotted lines.

Hydrogen-bonded assemblies of 1

The diboronic acid **1** was then recrystallized from THF/*n*-hexane to afford deep and light orange single crystals, named Forms I and II, respectively, suitable for X-ray diffraction (XRD) analysis. The molecular structure of **1** in the crystal of Form I is shown in Fig. 1. The two Cp rings in the fulvalenide moiety are coplanar; one iron ion is above the fulvalenide plane and the other is below it, as is common for most BiFc derivatives.[12] While 1,1'-disubstituted ferrocene derivatives can acquire various conformations because of the rotational flexibility whose ideal conformations are shown in Chart 1,[15] both ferrocenyl groups of **1** showed a nearly "synperiplanar eclipsed" conformation of the B(OH)$_2$ and Cp substituents, resulting in a transoid arrangement of the B(OH)$_2$ groups in **1** (a torsion angle of 0° for C5-B1-B1^1-C5^1) so that the B(OH)$_2$ substituents can be located at the position above the Cp ring of the other sandwich. This conformation is advantageous for forming an oriented assembly. Indeed, each molecule of **1** connects with the neighbouring two molecules through hydrogen bonds to afford a 1D hydrogen-bonded network, *i.e.*, chain, as shown in Fig. 2a. In the chain, a B(OH)$_2$ group of **1** provides a H atom and an O atom to an adjacent B(OH)$_2$ group for hydrogen-bond formation to form an octaatomic ring as shown in Fig. 3. The octaatomic ring is almost coplanar and the O–O distance between molecules (O1–O2^1) is 2.7936(19) Å. The two remaining H atoms (H2) do not participate in hydrogen-bond formation; the O–O distances between neighbouring chains (O1–O2^2 3.491(2)) are larger than those inside chains and those for usual OH···O hydrogen bonds[16] (Fig. S9) but shorter than the sum of the van der Waals radii, making short contacts (H2^2–O1).

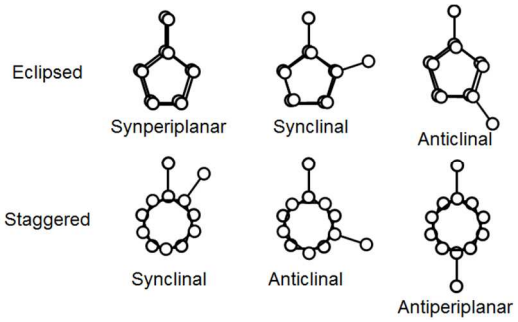

Chart 1 Ideal conformations of the ferrocenyl rings in 1,1′-disubstituted ferrocenes.[15]

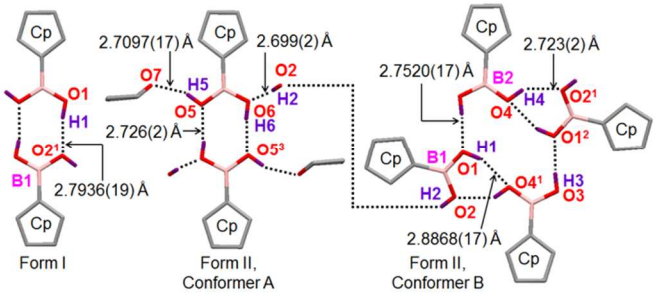

Fig. 3 Schematic representation of octaatomic and dodecaatomic rings in the crystals of Forms I and II.

The crystal of Form II had a composition of $(\mathbf{1})_3(THF)_2$ and the molecular structures are shown in Fig. S10. In the solvated crystals, **1** exists in two conformers with respect to the rotation of the $CpB(OH)_2$ moieties relative to the Cp rings of the fulvalenide moieties; Conformer A is nearly "synperiplanar eclipsed" while Conformer B shows both nearly "synperiplanar eclipsed" and "anticlinal eclipsed" conformations. As shown in Figs. 2b and 3, Conformer A formed hydrogen-bonded networks (O5–O6[3] 2.726(2) Å) similar to those in the non-solvated crystal (see Fig. 1a), although one difference is that the two remaining H atoms of the $B(OH)_2$ groups formed lateral hydrogen bonds with THF molecules (O5–O7 2.7097(17) Å). Conformer B formed dimers having hexaatomic rings through double hydrogen bonds (O1–O4[1] 2.8868(17) Å, O4-O2[1] 2.723(2) Å) of each of the $B(OH)_2$ groups; the obtained dimers were assembled by additional hydrogen bonds (O3–O1[2] 2.7520(17) Å) to form dodecaatomic rings, as shown in Figs. 1b and 3. The dodecaatomic rings were connected to hexaatomic rings on both sides to form a new planar hydrogen-bonded motif involving four $B(OH)_2$ groups. As a result, stepwise laminated networks of the planar motif were constructed. In addition to these four different hydrogen-bond arrangements, the remaining H atoms (H2) of the latter conformers form further hydrogen bonds (O2–O6 2.699(2) Å) to assemble the 1D and stepwise networks (Fig. S11). These results reveal the diversity of hydrogen-bonding motifs of $B(OH)_2$ groups introduced in a flexibly rotating double-sandwich geometry; in contrast, in a single-sandwich counterpart **B** only a chain criss-cross motif was observed.[11a]

Covalent-bonded assembly of 1

To obtain a covalent-bonded assembly, **1** was reacted with one equivalent of pentaerythritol (**P**), a tetraol linking agent, in acetone at 80 °C in a sealed tube. MALDI-TOF-MS analysis revealed that the resulting orange crude product contains

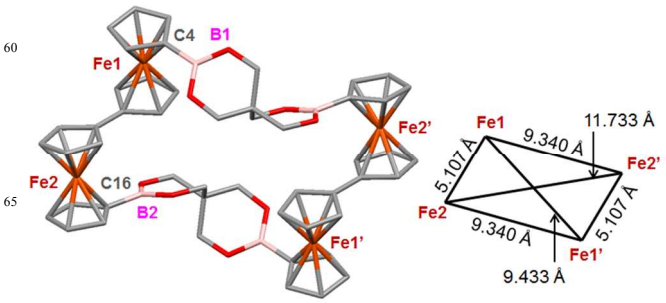

Fig. 4 Crystal structure of **2**. Hydrogen atoms are omitted for clarity. Fe-Fe distances are also shown.

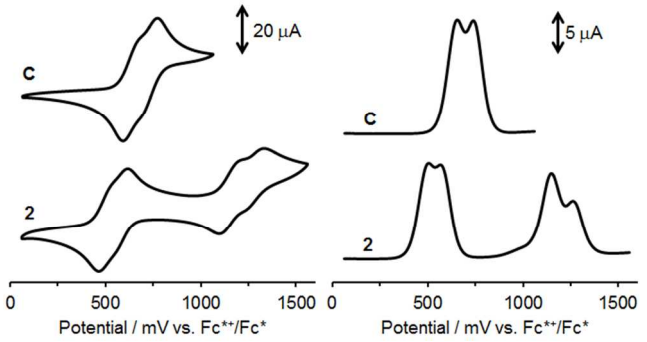

Fig. 5 Cyclic voltammograms (left) and differential pulse voltammograms (right) of **2** and **C** (1.0 mM) in CH_2Cl_2 containing *n*-Bu_4NBArF (0.1 M). Scan rate: 100 mV s^{-1}; [**2**] = [**C**] = 1.0 mM.

Table 1. Redox potentials $E_{1/2}{}^n$ and comproportionation constants K_n for **2** and **C**.[a]

Compound	$E_{1/2}{}^1$	$E_{1/2}{}^2$	$E_{1/2}{}^3$	$E_{1/2}{}^4$	K_1	K_2	K_3
2	528	585	1169	1284	9.2	7.5 x 10^9	88
C	674	756	-	-	24	-	-

[a] Potentials in mV vs. Fc^{*+}/Fc^* (Fc^* = decamethylferrocene). The values of K_n were determined by eq. 3 in Experimental Section.

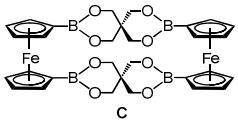

C

oligomers having $[FcFcBO_2C_5H_8O_2B]$ repeat units (n = 2 ~ 6) as shown in Fig. S4. The chemical formula $[FcFcBO_2C_5H_8O_2B]_n$ corresponds to cyclic oligomers. Interestingly, most observed peaks were assigned to the cyclic oligomers rather than $B(OH)_2$ or CH_2OH terminated linear oligomers. This selectivity to cyclic compounds is reasonable because **P** serves as a twisted linker rather than linear one (see the B···C(spiro)···B angle in the two dioxaborane rings below). Extraction of the resulting orange solid with $CHCl_3$ and crystallization from $CHCl_3$/diethyl ether afforded compound **2** in 33% yield. Identification by ^{11}B-, ^1H- and ^{13}C-NMR, ESI-MS (Figs. S5–8) and XRD confirmed that **2** is a macrocyclic dimer. The solid-state molecular structure of **2** is shown in Fig. 4. Fe(II) ions of **2** are located at four apexes of a parallelogram. Unlike the transoid arrangement of the $B(OH)_2$ groups in **1**, ferrocenyl groups of **2** showed nearly "synperiplanar and synclinal eclipsed" conformations of the $B(OH)_2$ and Cp substituents, resulting in a torsion angle of −68.55° for B1-C4-C16-B2. In **2**, the B···C(spiro)···B angle o(130.45°) is 7.15° smaller than that found in the reference macrocyclic dimer

composed of **B** and **P** ([$FcBO_2C_5H_8O_2BFc]_2$ (**C**)), as reported by Aldridge *et al*..[11b] This distorted structure of the dioxaborane rings in **2** increased the twist angle between the Cp rings in the fulvalenide moiety (11.7°). In $CDCl_3$ and DMSO-d_6, eight CH_2 protons were equivalent in the ^{1}H-NMR measurements of **2**, implying its symmetric structure in solution. In the DFT optimized geometry of **2** using the B3LYP/LanL2DZ (Fe atom) and 6-31G(d) (all other atoms) levels of theory, Fe(II) ions of **2** are also located at four apexes of a parallelogram as shown in Fig. S13 and Table S4 while the Fe···Fe distances between the BiFc units and the twisted angle between the Cp rings in the fulvalenide moieties are enlarged because of the absence of crystal-packing effects compared to those determined by XRD analysis (Table S8). To the best of our knowledge, **2** is the first macrocyclic compound composed of BiFc units, although several macrocyclic compounds composed of Fc units and heteroatom spacers have been reported.[17]

The electrochemical behaviour of **2**, together with that of the reference macrocycle **C**, was investigated using cyclic voltammetry (CV) and differential pulse voltammetry (DPV) in CH_2Cl_2 containing *n*-Bu_4NBArF_4 (ArF = 3,5-bis(trifluoromethyl) phenyl) at 298 K as shown in Fig. 5. The data are listed in Table 1. Compound **2**, which has four chemically equivalent ferrocenyl units, exhibited four defined reversible waves with a total spread of 756 mV ($E_{1/2}^4 - E_{1/2}^1$), indicating interactions between the four ferrocenyl units. The large redox splitting between $E_{1/2}^2$ and $E_{1/2}^3$ for **2** gave a 10^9 order thermodynamic stability for $\mathbf{2}^{2+}$, in which the two ferrocenium sites are located on the longer diagonal of the parallelogram; this would be favoured electrostatically, as shown in Scheme 2. This large stabilization primarily comes from the electronic interactions inside the BiFc units. This is consistent with the DFT calculations for **1**, **2** and **C** (Figs. S12–14, Tables S2–7); the HOMO and HOMO–1 in **2** are delocalized across the iron centres through p_z orbitals of the fulvalenide rings but not across the $BO_2C_5H_8O_2B$ linkers, retaining the properties of HOMOs of **1** and **C** (Fig. S15). While **C** exhibited two defined waves indicative of the electrostatic interaction between Fc units across the dioxaborane rings ($E_{1/2}^2 - E_{1/2}^1 = 82$ mV), **2** exhibited a smaller redox splitting between $E_{1/2}^1$ and $E_{1/2}^2$ (57 mV). This result confirmed the electrostatic interaction between the BiFc units across the dioxaborane rings in **2** although this interaction is weaker than that in **C** because of the difference in macrocycle size, consistent with the DFT-optimized Fe-Fe distances (12.19 Å for **2** in the longer diagonal, 9.68 Å for **C**). The comproportionation constant for $\mathbf{2}^{3+}$ (K_3) is larger by factors of 3.7 and 9.6 than those for $\mathbf{C}^+$ (K_1) and $\mathbf{2}^+$ (K_1), respectively, reflecting the greater thermodynamic stability of $\mathbf{2}^{3+}$ and the larger electrostatic repulsion upon formation of the highly charged species $\mathbf{2}^{4+}$. It should be noted that assembling Fe(II) ions with two types of ligands (CpCp and $CpBO_2C_5H_8O_2BCp$) afforded two types of interactions (strong through-bond and weak through-space) inside the discrete tetra-ferrocenyl complex **2**.

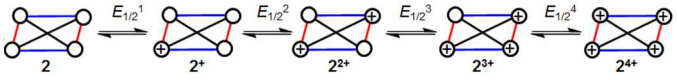

Scheme 2. Graphical representation of the electrochemical behaviour of **2**. Each circle represents a ferrocenyl unit.

Conclusions

A new organobimetallic complex **1** forms 1D hydrogen-bonded networks with or without lateral hydrogen bonds with solvent molecules, as well as a stepwise laminated network. This boronic acid-based supramolecular method provides new insight into association of functional bimetallic complexes without additional metal-ligand coordination chemistry. A cyclocondensed dimeric compound **2** between the flexible building block **1** and a rigid tetraol linker (pentaerythritol) exhibited unique electrochemical behaviour, showing both intra- and inter-biferrocenyl interactions, in sharp contrast to previously reported macrocyclic multiferrocenyl compounds,[16] which display only electrostatic interactions.

Experimental

Materials and methods

All solvents and chemicals used in the syntheses were of reagent grade and were used without further purification. 1′,1‴-Dibromobiferrocene,[14] **C**,[11b] and *n*-Bu_4NBArF[18] were synthesized according to previously reported procedures.

The UV-vis-NIR absorption spectra were measured on a JASCO V-670 spectrometer at room temperature. The ^{1}H-, ^{13}C{^{1}H}-, and ^{11}B-NMR spectra were recorded using JEOL JNM-ECP400 and JNM-ECA600 spectrometers installed at the Nara Institute of Science and Technology; tetramethylsilane (TMS) was used as an internal standard (0 ppm) for ^{1}H- and ^{13}C{^{1}H}-NMR analysis and $Et_2O{\cdot}BF_3$ was used as an external standard (0 ppm) for ^{11}B-NMR analysis. The ESI-MS were obtained using a JEOL JMS-T100CS spectrometer. The MALDI-TOF-MS were obtained using a Bruker Autoflex II spectrometer). Elemental analyses were performed using a Perkin Elmer 2400 II CHNS/O elemental analyzer.

All voltammetric experiments were carried out using a BAS electrochemical analyzer (Bioanalytical Systems Inc, West Lafayette, IN, USA). All experiments were performed using a conventional three-electrode system at 298 K. A platinum wire (1.6 mm diameter) was employed as the counter electrode, a glassy carbon electrode (3.0 mm diameter) as the working electrode and an Ag-AgCl (3.0 M NaCl) electrode as the reference electrode. Typically, nonaqueous CH_2Cl_2 solutions containing **2** and *n*-Bu_4NBArF_4 (0.1 M) were deaerated prior to each measurement, and an argon atmosphere was maintained inside the cell throughout each measurement. Each experiment was first performed in the absence of any internal standard and then repeated in the presence of decamethylferrocene (Fc*). A separate experiment containing only ferrocene and decamethylferrocene was also performed. The potentials are quoted relative to Fc^{*+}/Fc* couple. In this setup, the Fc^+/Fc couple was observed at 618 mV *vs.* Fc^{*+}/Fc* while the Fc^+/Fc couple was at 568 mV *vs.* Ag/AgCl in CH_2Cl_2/*n*-Bu_4NBArF. The potential data quoted relative to the Fc^+/Fc couple are also shown in Table S1. Compounds **2** and **C** had multiple redox potentials, as described by eq. 1. When $\mathbf{A}^{n+}$ is in equilibrium with species $\mathbf{A}^{n-1}$ and $\mathbf{A}^{n+1}$ (eq. 2), the comproportionation constant K_n can be obtained from $\Delta E = E_{1/2}^{n+1} - E_{1/2}^{n}$ (eq. 3), where F is Faraday's constant.

Table 2 Summary of crystallographic data and refinement parameters for **1**, $(\mathbf{1})_3(THF)_2$ and **2**.

	1	$(\mathbf{1})_3(THF)_2$	**2**
empirical formula	$C_{20}H_{20}B_2Fe_2O_4$	$C_{68}H_{76}B_6Fe_6O_{14}$	$C_{50}H_{48}B_4Fe_4O_8$
formula weight	457.69	1517.28	1043.55
crystal dimensions (mm)	0.120 x 0.040 x 0.030	0.130 x 0.090 x 0.030	0.110 x 0.030 x 0.020
crystal system	monoclinic	monoclinic	monoclinic
space group	$P2_1/n$ (#14)	C2/c (#15)	$P2_1/n$ (#14)
temperature (°C)	−150	−150	−150
a (Å)	5.6275(1)	29.2155(6)	8.4782(2)
b (Å)	19.4131(4)	8.7788(2)	10.0863(2)
c (Å)	8.1555(2)	27.5805(5)	25.0146(5)
β (deg)	105.4700(7)	114.5886(7)	91.4018(7)
V (Å^3)	858.69(3)	6432.3(2)	6432.3(2)
Z	2	4	2
ρ_{calcd} (g cm^{-3})	1.770	1.567	1.621
F(000)	468.00	3128.00	1072.00
μ (MoK$_\alpha$) (cm^{-1})	17.139	13.831	13.876
$2\phi_{max}$ (deg)	55.0	55.0	55.0
GOF	1.193	1.134	1.142
R1[a]	0.0289	0.0324	0.0286
wR2[b]	0.0836	0.0880	0.0765
$\Delta\rho_{max}/\Delta\rho_{min}$ (e/Å^3)	0.70/−0.43	1.08/−0.47	0.72/−0.33

[a] $R1 = \Sigma \, ||F_o| - |F_c|| \, / \, \Sigma \, |F_o|$. [b] $wR2 = [\Sigma \, (w(F_o^2 - F_c^2)^2) / \Sigma \, w(F_o^2)^2]^{1/2}$.

$$\mathbf{A^{n-1}} \xrightarrow[-e^-]{E_{1/2}^{n}} \mathbf{A^{n+}} \xrightarrow[-e^-]{E_{1/2}^{n+1}} \mathbf{A^{n+1}} \quad (1)$$

$$\mathbf{A^{n-1}} + \mathbf{A^{n+1}} \xrightarrow{K_n} 2\,\mathbf{A^{n+}} \quad (2)$$

$$K_n = [\mathbf{A^{n+}}]^2/[\mathbf{A^{n-1}}][\mathbf{A^{n+1}}] = \exp(\Delta E\, F/RT) \quad (3)$$

Synthesis of 1′,1‴-biferrocenediboronic acid (1)

1′,1‴-Dibromobiferrocene (0.306 g, 0.579 mmol) was dissolved in dry THF (15 ml). After the addition of an *n*-hexane solution of *n*-butyllithium (1.6 M, 1.1 ml) at −78 °C, the reaction mixture was stirred for 1 h. Then, tributyl borate (0.412 g, 1.79 mmol) was added to the reaction mixture. After stirring overnight, an aqueous solution of KOH (10%, 5 ml) was added. After stirring for 10 min, the reaction mixture was extracted with an aqueous solution of KOH (10%, 45 ml). Upon addition of 10% sulphuric acid at 0 °C, a dark brown reprecipitate was filtered and suspended in $CHCl_3$. The target compound was obtained by filtration as an orange solid. Yield: 671 mg (76%). Mp.: >250 °C. ^{1}H-NMR (600 MHz, DMSO-d_6, ppm): δ = 4.01 (pt, 4H, C_4H_4), 4.04 (pt, 4H, C_4H_4), 4.23 (pt, 4H, C_4H_4), 4.32 (pt, 4H, C_4H_4), 7.37 (s, 4H, O*H*). ^{13}C-NMR (150 MHz, DMSO-d_6, ppm): δ = 64.90 (*C*-B(OH)$_2$), 66.73, 67.89, 72.29, 74.25, 83.74 (*C*-C_5H_5). ^{11}B-NMR (128 MHz, DMSO-d_6, ppm): δ = 28.96 (br). HR-ESI-MS (m/z). Calc. for $C_{20}H_{20}B_2Fe_4O_4$ [M^+]: 458.0255. Found: 458.0225. UV-vis (DMSO): [λ_{max}/nm] (ε_{max}), 301 (7.38 × 10^3), 452 (650).

Synthesis of [FcFcBO$_2$C$_5$H$_8$O$_2$B]$_2$ (2)

A mixture of **1** (202 mg, 0.442 mmol) and pentaerythritol (60 mg, 0.44 mmol) in dry acetone (15 ml) was sealed in a thick-walled pressure tube and stirred at 80 °C for 16 h. After filtration of the solution, the orange residue was dried in vacuo. The residue was dispersed in $CHCl_3$ and the filtrate was evaporated to dryness to give the target compound. Yield: 75 mg (33%). HR-ESI-MS (m/z). Calc. for $C_{50}H_{48}B_4Fe_4O_8$ [M^+]: 1044.1134. Found: 1044.1153. ^{1}H-NMR (600 MHz, DMSO-d_6, ppm): δ = 4.03 (s, 2H, CH_2), 4.08 (pt, 1H, C_4H_4), 4.17 (pt, 1H, C_4H_4), 4.20 (pt, 1H, C_4H_4), 4.45 (pt, 1H, C_4H_4). ^{1}H-NMR (600 MHz, $CDCl_3$, ppm): δ = 4.01 (s, 2H, CH_2), 4.22 (m, 3H), 4.40 (pt, 1H). ^{13}C-NMR (150 MHz, $CDCl_3$, ppm): δ = 36.58 (*C*(spiro)), 64.80 (CH_2), 66.79, 68.08, 72.98, 74.49, 84.02 (*C*-C_5H_5). ^{11}B-NMR (400 MHz, $CDCl_3$, ppm): δ = 28.60 (br). UV-vis (CH_2Cl_2): [λ_{max}/nm] (ε_{max}), 298 (1.56 x 10^4), 456 (1.43 x 10^3).

Single crystal X-ray diffraction (XRD) analysis

Single crystals of **1** and $(\mathbf{1})_3(THF)_2$ suitable for XRD analysis were obtained by diffusion of hexane into a THF solution containing **1** at ambient temperature. Single crystals of **2** for XRD analysis were obtained by diffusion of ether into a $CHCl_3$ solution containing **1** at ambient temperature. Data were collected with a Rigaku ValiMax RAPID RA-Micro7HFM using Mo Kα radiation at −150 °C. The diffraction data were processed with RAPID AUTO on a Rigaku program, and the structures were solved by direct methods and refined on F^2 by full-matrix least-squares using CrystalStructure and SHELXL-97 (Table 2). CCDC 982376, 982377 and 982378 contain the supplementary crystallographic data for **1**, $(\mathbf{1})_3(THF)_2$ and **2** in this paper, respectively. These data can be obtained free of charge from the Cambridge Crystallographic Data Centre via www.ccdc.cam.ac.uk/data_request/cif.

DFT calculations

The calculations were carried out using the Gaussian09 program package.[19] The geometries of **1**, **2** and **C** were optimised using

DFT methods without symmetry constraints. The three-parameterized Becke–Lee–Yang–Parr (B3LYP) hybrid exchange-correlation functional[20] was used with the Lanl2DZ (Hay–Wadt ECP) basis set[21] for the Fe atom and the 6-31G(d) basis set[22] for the other atoms; solvent effects were not taken into account. The stability of the optimised gas-phase structure was confirmed by calculating the molecular vibrational frequencies, in which no imaginary frequencies were observed. The single-point calculations were carried out using the same basis set as used for the geometry optimisations, also without considering solvent effects. Molecular composition analysis was conducted using the GaussSum Program. In the optimised structures of **2** and **C**, ferrocenyl groups showed nearly eclipsed conformations of the $B(OH)_2$ and Cp substituents (Tables S4 to S7 and Figs. S13 and 14). For **1**, an optimised structure with a nearly eclipsed conformation and that with a more staggered conformation (**1'**) were obtained as shown in Fig. S11. Although the latter is the most stable structure in gas-phase, we adopted the former (Tables S2 and S3 and Fig. S15) to discuss inter-ferrocenyl interactions of **1**, **2** and **C** in the same nearly eclipsed conformation.

Acknowledgements

This work was partially supported by a Grant-in-Aid for Young Scientists B (No. 25790016) and a research grant from the Murata Science Foundation. The authors would like to thank Mr. Fumio Asanoma and Ms. Yoshiko Nishikawa (NAIST) for the NMR and ESI-MS measurements, respectively.

Notes and references

[a] *Graduate School of Materials Science, Nara Institute of Science and Technology (NAIST), 8916-5, Takayama, Ikoma, Nara 6300192, Japan. E-mail: taharak@ms.naist.jp*

[b] *Division of Liberal Arts, Kogakuin University, 2665-1, Nakano, Hachioji, Tokyo 1920015, Japan.*

† Electronic Supplementary Information (ESI) available: Synthesis, characterisation, DFT calculation of **1** and **2**. CCDC 982376-982378. See DOI:10.1039/b000000x/

1 For selected reviews, see: (a) O. M. Yaghi, M. O'Keeffe, N. W. Ockwig, H. K. Chae, M. Eddaoudi and J. Kim, *Nature*, 2003, **423**, 705-714; (b) S. Kitagawa, R. Kitaura and S. Noro, *Angew. Chem. Int. Ed.*, 2004, **43**, 2334-2375; (c) M. Yoshizawa, J. K. Klosterman and M. Fujita, *Angew. Chem. Int. Ed.*, 2009, **48**, 3418 – 3438.

2 (a) I. AmLani, A. O. Orlov, G. Toth, G. H. Bernstein, C. S. Lent and G. L. Snider, *Science*, 1999, **284**, 289-291; (b) C. S. Lent, *QUANTUM CELLULAR AUTOMATA Theory, Experimentation and Prospects*, ed. M. Macucci, Imperial College Press, London, 2006, pp. 269-276.

3 (a) C. S. Lent, B. Isaksen and M. Lieberman, *J. Am. Chem. Soc.*, 2003, **125**, 1056-1063; (b) H. Qi, S. Sharma, Z. Li, G. L. Snider, A. O. Orlov, C. S. Lent and T. P. Fehlner, *J. Am. Chem. Soc.*, 2003, **125**, 15250-15259; (c) K. Tokunaga, *Chem. Phys. Phys. Chem.*, 2009, **11**, 1474-1483; (d) K. Tokunaga, *Materials*, 2010, **3**, 4277-4290; (e) X. Wang, S. Chen, J. Wen and J. Ma, *J. Phys. Chem. C*, 2013, **117**, 1308-1314.

4 For selected examples, see: (a) C. P. Kubiak, *Inorg. Chem.*, 2013, **52**, 5663−5676; (b) P.-C. Lin, H.-Y. Chen, P.-Y. Chen, M.-H. Chiang, M. Y. Chiang, T.-S. Kuo and S. C. N. Hsu, *Inorg. Chem.*, 2011, **50**, 10825−10834.

5 (a) *Boronic Acids: Preparation and Applications in Organic Synthesis, Medicine and Materials*, ed. D. G. Hall, Wiley-VCH, 2011; (b) K. Severin, *Dalton Trans.*, 2009, 5254-5264; (c) R. Nishiyabu, Y. Kubo, T. D. James and J. S. Fossey, *Chem. Commun.,* 2011, **47**, 1124–1150; (d) R. Nishiyabu, Y. Kubo, T. D. James and J. S. Fossey, *Chem. Commun.*, 2012, **47**, 1106-1123; (d) N. A. Celis, C. Godoy-Alcántar, J. Guerrero-Álvarez and V. Barba, Eur J. Inorg. Chem., 2014, 1477-1484.

6 (a) A. P. Côté, A. I. Benin, N. W. Ockwig, M. O'Keeffe, A. J. Matzger, O. M. Yaghi, Science, 2005, 310, 1166-1170; (b) A. L. Korich and P. M. Iovine, *Dalton Trans.*, 2010, **39**, 1423-1431.

7 (a) R. Nishiyabu, S. Teraoka, Y. Matsushima and Y. Kubo, *ChemPlusChem,* 2012, **77**, 201-209; (b) R. Nishiyabu, Y. Sugino and Y. Kubo, *Chem. Commun.,* 2013, **49**, 9868-9871.

8 For selected recent examples, see: (a) S. Ito, K. Ono and N. Iwasawa, *J. Am. Chem. Soc.*, 2012, **134**, 13962−13965; (b) M. Pascu, A. Ruggi, R. Scopelliti and K. Severin, *Chem. Commun.,* 2013, **49**, 45-47.

9 (a) K. E. Maly, T. Maris and J. D. Wuest, *CrysEngComm*, 2006, **8**, 33-35; (b) J. H. Fournier, T. Maris, J. D. Wuest, W. Z. Guo and E. Galoppini, *J. Am. Chem. Soc.*, 2003, **125**, 1002-1006; (c) C. J. Davis, P. T. Lewis, D. R. Billodeaux, F. R. Fronczek, J. O. Escobedo and R. M. Strongin, *Org. Lett.*, 2001, **3**, 2443-2445; (d) K. E. Maly, N. Malek, J.-H. Fournier, P. Rodríguez-Cuamatzi, T. Maris and J. D.Wuest, *Pure Appl. Chem.*, 2006, **78**, 1305-1321.

10 (a) C. Bresner, S. Aldridge, I. A. Fallis and L.-L. Ooi, *Acta Crystallogr., Sect. E: Struct. Rep. Online*, 2004, **E60**, m441–m443; (b) J. K. Day, A. L. Thompson and S. Aldridge, *J. Chem. Crystallogr.*, 2010, **40**, 156-159.

11 (a) D. Braga, M. Polito, M. Bracaccini, D. D'Addario, E. Tagliavini, L. Sturba, F. Grepioni, *Organometallics*, 2003, **22**, 2142–2150; (b) J. K. Day, C. Bresner, I. A. Fallis, L-L. Ooi, D. J. Watkin, S. J. Coles, L. Male, M. B. Hursthouse and S. Aldridge, *Dalton Trans.*, 2007, 3486-3488; (c) T.-H. Chen, W. Kaveevivitchai, N. B. and O. Š . Miljanić, *Chem. Commun.*, 2012, **48**, 2855–2857.

12 For selected examples, see: (a) D. O. Cowan and F. Kaufman, *J. Am. Chem. Soc.*, 1970, **92**, 6198–6204; (b) C. LeVanda, K. Bechgaard, D. O. Cowan and M. D. Rausch, *J. Am. Chem. Soc.*, 1977, **99**, 2964–2968; (c) T. Y. Dong, D. N. Hendrickson, K. Iwai, M. J. Cohn, S. J. Geib, A. L. Rheingold, H. Sano, I. Motoyama, S. Nakashima, *J. Am. Chem. Soc.*, 1985, **107**, 7996–8008; (d) R. J. Webb, T. Y. Dong, C. G. Pierpont, S. R. Boone, R. K. Chadha, D. N. Hendrickson, *J. Am. Chem. Soc.*, 1991, **113**, 4806–4812; (e) S. Nakashima, Y. Ueki, H. Sakai and Y. Maeda, *J. Chem. Soc., Dalton Trans.*, 1996, 139-143; (f) T-Y. Dong, M-C. Lin, L. Lee, C-H. Cheng, S-M. Peng and G-H. Lee, *J. Organomet. Chem.*, 2003, **679**, 181-193; (g) T. Y. Dong. T. Kambara and D. N. Hendrickson, *J. Am. Chem. Soc.*, 1986, **108**, 5857–5865; (h) S. Nakashima, T. Oda, T. Okuda and M. Watanabe, *Inorg. Chem.*, 1999, **38**, 4005–4010; (i) T. Oda, S. Nakashima and T. Okuda, *Inorg. Chem.*, 2003, **42**, 5376–5383; (j) D. R. Talham and D. O. Cowan; *Organometallics*, 1987, **6**, 932–937; (k) W. Zhang, S. R. Wilson and D. N. Hendrickson, *Inorg. Chem.,* 1989, **28**, 4160-4165; (l) N. J. Long, A. J. Martin, R. Vilar and A. J. P. White, D. J. Williams and M. Younus, *Organometallics*, 1999, **18**, 4261-4269; (m) L. Xiao, W. Weissensteiner, K. Mereiter and M. Widhalm, *J. Org. Chem.*, 2002, **67**, 2206-2214; (n) N. Nagahora, S. Ogawa, Y. Kawai and R. Sato; *Tetrahedron Lett.*, 2005, **46**, 4157-4160; (o) M. Lohan, P. Ecorchard, T. Rüffer, F. Justaud, C. Lapinte and H. Lang; *Organometallics*, 2009, **28**, 1878–1890; (p) G. Espino, L. Xiao, M. Puchberger, K. Mereiter, F. Spindler, B. R. Manzano, F. A. Jalóne and W. Weissensteiner, *Dalton Trans.*, 2009, 2751-2763; (q) M. Lohan, F. Justaud, T. Roisnel, P. Ecorchard, H. Lang and C. Lapinte, *Organometallics*, 2010, **29**, 4804–4817; (r) M. Lohan, F. Justaud, H. Lang and C. Lapinte; *Organometallics*, 2012, **31**, 3565–3574; (s) A. Zirakzadeh, M. A. Groß, Y. Wang, K. Mereiter, F. Spindler and Walter Weissensteiner; *Organometallics*, 2013, **32**, 1075–1084.

13 (a) D. Siebler, C. Förster, T. Gasi and K. Heinze, *Organometallics*, 2011, **30**, 313–327; (b) M. Lohan, B. Milde, S. Heider, J. M. Speck, S. Krauße, D. Schaarschmidt,T. Ru□ffer and H. Lang, *Organometallics*, 2012, **31**, 2310-2326; (c) Y. Wang, A. Rapakousiou, G. Chastanet, L. Salmon, J. Ruiz and Di. Astruc, *Organometallics*, 2013, **32**, 6136-6146.

14 T.-Y. Dong, C.-K. Chang, S.-H. Lee, L.-L. Lai, M. Y.-N. Chiang and K.-J. Lin, *Organometallics*, 1997, **16**, 5816-5825.

15 N. Sadhukhan and J. K. Bera, *Inorg. Chem.*, 2009, **48**, 978-990.
16 (a) G. A. Jeffrey, *An Introduction to Hydrogen Bonding*, *Oxford University Press*, 1997, Oxford; (b) T. Steiner, *Angew. Chem., Int. Ed.*, 2002, **41**, 48-79.
17 For selected recent examples, see: (a) D. E. Herbert, J. B. Gilroy, W. Y. Chan, L. Chabanne, A. Staubitz, A. J. Lough and I. Manners, *J. Am. Chem. Soc.*, 2009, **131**, 14958-14968; (b) B. Bagh, N. C. Breit, K. Harms, G. Schatte, I. J. Burgess, H. Braunschweig and J. Müller, *Inorg. Chem.*, 2012, **51**, 11155-11167; (c) B. Bagh, N. C. Breit, S. Dey, J. B. Gilroy, G. Schatte, K. Harms and J. Müller, *Chem. –Eur. J.*, 2012, **18**, 9722-9733; (d) S. Bruña, A. M. González-Vadillo, D. Nieto, C. J. Pastor and I. Cuadrado, *Macromolecules*, 2012, **45**, 781−793; (e) B. Bagh, N. C. Breit, J. B. Gilroy, G. Schattec and J. Müller, *Chem. Commun.*, 2012, **48**, 7823–7825.
18 F. Barrière and W. E. Geiger, *J.Am. Chem. Soc.*, 2006, **128**, 3980-3989.
19 M. J. Frisch, G. W. Trucks, H. B. Schlegel, G. E. Scuseria, M. A. Robb, J. R. Cheeseman, G. Scalmani, V. Barone, B. Mennucci, G. A. Petersson, H. Nakatsuji, M. Caricato, X. Li, H. P. Hratchian, A. F. Izmaylov, J. Bloino, G. Zheng, J. L. Sonnenberg, M. Hada, M. Ehara, K. Toyota, R. Fukuda, J. Hasegawa, M. Ishida, T. Nakajima, Y. Honda, O. Kitao, H. Nakai, T. Vreven, J. A. Montgomery, Jr., J. E. Peralta, F. Ogliaro, M. Bearpark, J. J. Heyd, E. Brothers, K. N. Kudin, V. N. Staroverov, R. Kobayashi, J. Normand, K. Raghavachari, A. Rendell, J. C. Burant, S. S. Iyengar, J. Tomasi, M. Cossi, N. Rega, J. M. Millam, M. Klene, J. E. Knox, J. B. Cross, V. Bakken, C. Adamo, J. Jaramillo, R. Gomperts, R. E. Stratmann, O. Yazyev, A. J. Austin, R. Cammi, C. Pomelli, J.W. Ochterski, R. L.Martin, K.Morokuma, V. G. Zakrzewski, G. A. Voth, P. Salvador, J. J. Dannenberg, S. Dapprich, A. D. Daniels, Ö. Farkas, J. B. Foresman, J. V. Ortiz, J. Cioslowski and D. J. Fox, Gaussian 09, Gaussian, Inc., Wallingford, CT, 2009.
20 D. Becke, *J. Chem. Phys.*, 1993, **98**, 5648-5652.
21 P. Hay, W.R. Wadt, *J. Chem. Phys.*, 1985, **82**, 270–273.
22 P. C. Hariharan, J. A. Pople, *Theor. Chim. Acta*, 1973, **28**, 213−222.

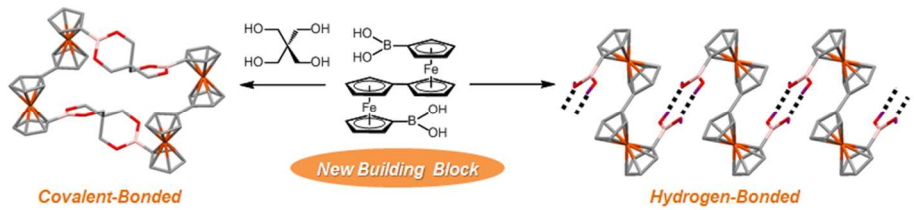

Covalent- and hydrogen-bonded assemblies were constructed from 1′,1′′′-biferrocenediboronic acid as a new organobimetallic building block.
242x50mm (96 x 96 DPI)